Simultaneous Visual Context-aware Path Prediction

Haruka Iesaki[1], Tsubasa Hirakawa[1], Takayoshi Yamashita[1], Hironobu Fujiyoshi[1], Yasunori Ishii[2], Kazuki Kozuka[2] and Ryota Fujimura[2]

[1]*Computer Science, Chubu University, 1200 Matsumoto-cho, Kasugai, Aichi, Japan*

[2]*Panasonic Corporation, Japan*

{*iesaki, hirakawa*}*@mprg.cs.chubu.ac.jp*, {*takayoshi, fujiyoshi*}*@isc.chubu.ac.jp*

Keywords: Path Prediction, Visual Forecasting, Predictions by Dashcams, Convolutional LSTM.

Abstract: Autonomous cars need to understand the environment around it to avoid accidents. Moving objects like pedestrians and cyclists affect to the decisions of driving direction and behavior. And pedestrian is not always one-person. Therefore, we must know simultaneously how many people is in around environment. Thus, path prediction should be understanding the current state. For solving this problem, we propose path prediction method consider the moving context obtained by dashcams. Conventional methods receive the surrounding environment and positions, and output probability values. On the other hand, our approach predicts probabilistic paths by using visual information. Our method is an encoder-predictor model based on convolutional long short-term memory (ConvLSTM). ConvLSTM extracts visual information from object coordinates and images. We examine two types of images as input and two types of model. These images are related to people context, which is made from trimmed people's positions and uncaptured background. Two types of model are recursively or not recursively decoder inputs. These models differ in decoder inputs because future images cannot obtain. Our results show visual context includes useful information and provides better prediction results than using only coordinates. Moreover, we show our method can easily extend to predict multi-person simultaneously.

1 INTRODUCTION

Paths prediction is strongly required by many applications (e.g., autonomous driving, robot navigation, and congestion forecasts). In particular, there have been many studies on autonomous driving. Autonomous driving needs high precision performance in complex environments. Thus, scene understanding is needed to perceive the environment around the car. Scene understanding has rapidly progressed over the last few years. It has been used to interpret risky regions (Kozuka and Niebles, 2017), (Zeng et al., 2017a) and visual explanations (Fukui et al., 2019), (Xu et al., 2015). Scene understanding is needed for long-time prediction because vehicles move at high speed. But people are affected by many factors such as the scene environment, road signs, human-human interactions, and people's beliefs. Therefore, predicting the hidden states of people is necessary to predict people's paths. We represent the hidden state as the probability distributions from the driver's viewpoint for the future. Probability is the key to prevent collisions by predicting future action to ensure safe driving on the road because probability values can show how the risk in the prediction areas.

Inspired by representation-based scene understanding methods, we propose an approach to predict the paths of people (including pedestrians and cyclists) by using dashcams in long-time horizons with uncertainty estimates.

Our contributions are as follows:

- For scene understanding, previous methods are image generation, risky region interpretation, and visual explanation. We apply these methods to path prediction by using dashcams.
- The surrounding environment can represent various data types like bounding box, segmentation, and optical flow. We compare how using visual context images can improve prediction. We compare using visual context images with two types of image: RGB and optical flow.
- In the future prediction, we do not know how visual context images can obtain. We compare two types of model, which differ what context images input to the predictor.

2 RELATED WORK

2.1 Vector-based Predictions

Path prediction methods by using vectors have been proposed (Bhattacharyya et al., 2017), (Zhang et al., 2019), (Du et al., 2018), (Deo and Trivedi, 2018), (Kooij et al., 2014). These approaches use coordinates or velocities to indicate the movement of the prediction target as input data and prediction results. (Bhattacharyya et al., 2017) proposed an on-board path prediction method. This method inputs bounding box information into an encoder-decoder based network, and the output bounding box indicates the future target location in a set of image coordinates. They introduce odometry information (i.e., speed and angle) as additional inputs, which enables us to predict paths under a dynamic environment.

In contrast to the vector-based prediction methods, our method inputs image data representing target locations and probabilistically predicts target locations in each set of image coordinates. Our method can explain how visual contexts have effective information and how this is easily extended to predictions of multiple targets.

2.2 Image-based Predictions

Prediction methods using image data have also been proposed not only for path predicition problems (Rehder et al., 2017), (Makansi et al., 2019) but also another prediction problems (Palazzi et al., 2017), (Shi et al., 2015), (Bazzani et al., 2017). Image-based path prediction methods use feature values extracted by using a convolutional neural network (CNN) and the bounding boxes of the prediction targets as inputs. Then, these data are input to a deep neural network (DNN) (Hinton and Salakhutdinov, 2006), which predicts future target locations.

However, convoluted image data have many feature values. Thus, those feature values and bounding boxes inputted to the DNN cause a problem because the precious features of the bounding box disappear.

An effective obtainment from the image method has been proposed by using a probabilistic attention sight (Palazzi et al., 2017), (Bazzani et al., 2017), forecasting segmentation by using segmentation images (Luc et al., 2018), and probability prediction of mixture probability distribution with images made from trimmed people's positions (Makansi et al., 2019).

Methods to extract features from images have been proposed (Tran et al., 2015), (Shi et al., 2015), (Zeng et al., 2017b), (Hsieh et al., 2018). (Shi et al., 2015) proposed an encoder-predictor network which is also called encoding-forecasting structure. The encoder-predictor model consists of convolutional long short-term memory (ConvLSTM). ConvLSTM is a recursive learning method with requiring inputted image features. The ConvLSTM network we used is shown in Figure 1. The ConvLSTM consists of convolution layers and long term-short memory (LSTM) (Hochreiter and Schmidhuber, 1997). Learning by LSTM usually needs inputted vectors such as bounding box and odometry. On the other hand, ConvLSTM can use input images features. Input features x_t and previous hidden state's features h_{t-1} convolute, and these features are separated into four LSTM gates. ConvLSTM is able to extract image features and learn recursively. This network can robustly predict paths for time sequence behavior.

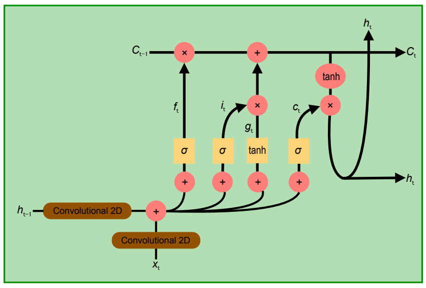

Figure 1: Convolutional Long Short-Term Memory (ConvLSTM).

Figure 2: Dataset sample image.

3 PROPOSED METHOD

In this paper, we propose probabilistic paths prediction by using captured dashcams images. We compare two types of image and two types of model and, evaluate probability rates and the error which of truth and prediction images. We explain the details of our proposed method. Our approach also does not depends on the number of people. Thus, we perform a one-person prediction experiment and a multi-person prediction experiment to verify this.

3.1 Context Images

The two types of image that are compared are RGB and optical flow. RGB images are the ordinary images captured by dashcams. Optical flow images only have information about movements surrounding objects. We use two types of image, which is made from trimmed people's positions, and the others background are uncaptured. They have only context about people's locations. A made image sample is shown in Figure 2.

3.2 Network Architectures

The two types of models that are compared have different inputted decoder images. In this section, a non-context image means black images.

Model 1
Model 1 is shown in Figure 3. A non-context image is inputted to predictor each time. This model only predict by using learned parameters in encoder. It means that how this model can predict from visual context in the past.

Model 2
model 2 is shown in Figure 4. This model is recursively input to predictor each time. The first prediction uses the last image of the encoder, and the others prediction use predicted images of each previous time. We verify how the input image in predictor effect to predict between the model 1 and model 2.

3.3 Training Loss

The training loss in learning time is the mean absolute error (MAE) between a truth image and a prediction image, as shown in Eq. 1. The number of prediction frames is F, the batch size is B, a truth image is y, and a prediction image is $\hat{y}$.

$$\mathrm{MAE} = \frac{1}{B}\frac{1}{F}\sum_{b=0}^{B}\sum_{f=0}^{F}(y,\hat{y})_f \tag{1}$$

4 EXPERIMENTS

First, we evaluate the one-person path prediction in 4.3. Second, we evaluate the multi-person path prediction in 4.4.

4.1 Dataset

Both of the experiments use the Cityscapes Dataset (Cordts et al., 2016). This dataset has first-person view video whose sequence of length 1.8 second (30 frames) obtained by dashcams and bounding boxes. The video resolution is 1024×2048 pixels. Bounding boxes is automatically annotated using tracking by detection method of (Tang et al., 2016). Annotation were obtained using the Faster R-CNN based method of (Zhang et al., 2017). The coordinates at the top left (x_1, y_1) and the bottom right (x_2, y_2) are shown for each person's position.

We also use the Oxford Town Centre dataset (Adam and Jules, 2019). We use only multi-person prediction for evaluating because multi-person is more complex problems. The dataset is a CCTV video, obtained from a surveillance camera, includes approximately 2,200 people.

We make context images by using images and bounding boxes, as explained in 3.1. There are three two of images: RGB and optical flow images converted by FlowNet 2.0 (Ilg et al., 2017). We does not use optical flow as vectors because we predict visual representation paths. We use optical flow color images which is converted vector to color. Them, these have 3 channels.

The optical flow rates are shown in Figure5a, 5b. This is only people's location rates of cityscapes dataset. This shows the target person's movements whose directions are represented by flow. We calculate the rate of eight directions, which are going counter clockwise, east-northeast (ENE), north-northeast (NNE), north-northwest (NNW), west-northwest (WNW), west-southwest (WSW), south-southwest (SSW), south-southeast (SSE), and east-southeast (ESE). This analysis shows optical flow rates does not differ on whether it is a one-person dataset or a multi-person dataset in training and testing.

4.2 Evaluation Metrics

In this paper, we evaluate the path prediction accuracy by using two performance indicators. We use negative log likelihood (NLL) (which indicates probability distribution error) and mean IoU (recall and precision).

The NLL evaluates the probabilistic differences between a prediction and true probability distribution. In our experiments, we normalize the output values to keep the property of probability distribution by using the maximum output values and evaluate one.

The mean IoU (mIoU) calculates the average rate of prediction probability in a truth bounding box and a prediction area. We evaluate it by using precision and recall rate. The precision rate is the rate of truth bounding box range to the predicted distribution. In contrast, the recall rate is the rate of predicted distribution to the truth bounding box range. High precision means predictive quality. And high recall means

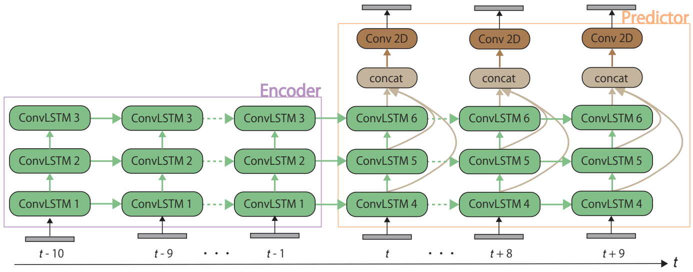

Figure 3: Model 1: Encoder is inputted context images. Predictor is inputted non-context images.

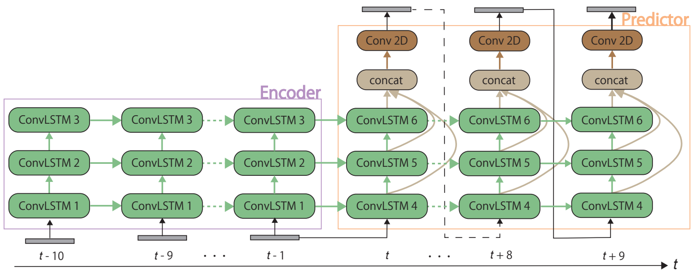

Figure 4: Model 2: Encoder is inputted context images. Predictor is inputted the last image of the encoder and predictions.

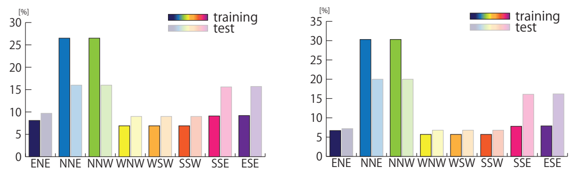

(a) One-person

(b) Multi-person

Figure 5: The distribution of optical flow in Cityscapes dataset. Each graph shows distributions of (a) one-person prediction and (b) multi-person prediction.

how well the prediction matches to the truth bounding box range, namely completeness. Each rates is calculated by using to the number of pixels over each threshold in the bounding box. The threshold range is from 0.0 to 1.0, which represents the probability.

4.3 One-person Prediction

First, we evaluate one-person prediction using the Cityscapes Dataset. The number of training samples is 6,792 videos, and the number of testing samples is 3,523 videos. The learning time is 10 epochs, and the mini-batch size is 2. We use the Adam optimizer, of which the learning rate is 0.001. Both input images (observation) and prediction images (future) are 10 frames. The images size is 128×256 pixels. In this experiment, we compare two types of model and two types of image.

Table 1: NLL of predictive distribution.

Method	Prediction frames	Image	NLL
LSTM-Bayesian	8	RGB	3.92
Our model 1	10	RGB	0.693
		Flow	**0.692**
Our model 2	10	RGB	0.693
		Flow	**0.692**

4.3.1 Probability Distribution Error

For evaluating the probability distribution error, we use the model of (Bhattacharyya et al., 2017) as a baseline model. The results are shown in Table 1. All of the results are lower than the baseline model. Among the images, using optical flow images lowered the error. It show the optical flow has effective movement context but the RGB images have noise context for prediction. However, it is not big different no matter what model to predict between models.

4.3.2 mIoU

The mIoU is shown in Figure 6a, 6b; the horizontal axis is the threshold range 0.0 to 1.0, and the vertical axis is the precision or recall rate in each bounding box average. The rate is calculated by the average over every prediction frame and the number of testing samples. From both results, the RGB images predict approximately the same lower probability in the bounding boxe area. On the other hand, optical flow images are able to predict higher probability in the

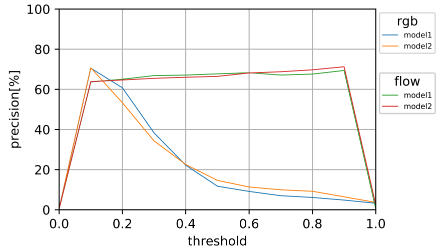

(a)

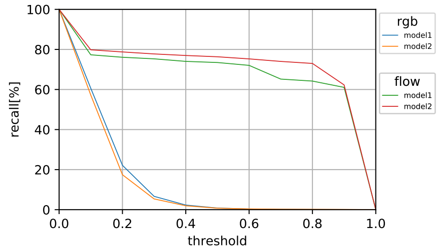

(b)

Figure 6: (a) Precision and (b) recall rates of one-person prediction on Cityscapes dataset.

bounding box area. In the models using flow image, recall is higher than precision when the threshold is between 0.1 and 0.9. It show that these model predict distribution close to truth bounding box area.

4.3.3 Visual Results for One-person

We show the only using optical flow images model in Figure 7, 8, which is the highest accuracy in Figure 6b. Model 1 leads to a lower prediction than model 2 in the first time of prediction, show in Figure 7. And Model 1 also predict distribution that is slightly larger than the true value region. On the other hand, Model 2 can predicts high probability distribution in the truth bounding box area. In path prediction, model 1 is also the lower prediction, shown in Figure 8 but both models predict approximately same paths. These results show that the recursive input images of predictor (model 2) effects better to non-recursive model (model 1) in the case of one-person prediction.

4.4 Multi-person Prediction

We also experiment on multi-person paths prediction. It is a more complex problem than one-person path prediction because people influence others objects. Therefor, we use the Cityscapes Dataset as we did for the one-person prediction and Oxford Town Centre Dataset. Cityscapes dataset's training samples are 1,978 videos, and the testing samples are 1,036 videos. The training conditions such as the learning time and the optimization are the same as those of the one-person prediction. Town Centre dataset's

Table 2: NLL of predictive distribution.

Method	Prediction frames	Image	NLL	
			Cityscapes	Town centre
LSTM-Bayesian	8	rgb	3.92	-
Our model 1	10	rgb	0.692	0.670
		flow	**0.690**	**0.650**
Our model 2	10	rgb	0.692	0.670
		flow	**0.690**	**0.650**

training samples are 135 videos, and the testing samples are 57 videos. The condition is also same as experiment using Cityscapes dataset, but image size is 135×240 pixels and the learning time is 200 epochs. We also compare two models (non-recursive and recursive predictor) and two types of image (RGB and optical flow).

4.4.1 Probability Distribution Error

Models using optical flow image are the lower error than the baseline model, show in Table 2. This does not show a big difference as to which model is suitable for prediction. However, using Town Centre dataset is lower than Cityscapes dataset. This is probably because Town Centre dataset is obtained by fixed camera, so there are no rapidly movement samples.

4.4.2 mIoU

The mIoU is shown in Figure 9a, 9b, 10a, 10b. As the results, RGB images predict almost the same low probability in bounding box area, show in Figure 9a, 9b. On the other hand, models using optical flow images predict high probability in bounding box area. In using optical flow models, the higher overlap rate is in the order of model 2, 1. These results show using recursively context image have the better effect on prediction than using non-context images. The models used Town Centre dataset is also almost same result, show in Figure 10a, 10b. However, predictions with low threshold is high recall for both models and images. This is thought to be because there is little information on movement by flow obtained from the bird's-eye view.

4.4.3 Visual Results for Multi-person Prediction

We show the only using optical flow images model in Figure 11, 12, 13, 14, which is the highest accuracy in Figure 9b, 10b. Figure 11, 12 are the results of Cityscapes dataset. Figure 13, 14 are the results of Town Centre dataset. Figure 11, 13 show the probability prediction with truth bounding boxes for each time. Figure 12, 14 show path predictions with path defined the truth bottom bounding boxes as truth paths. Both models gradually decrease the probability

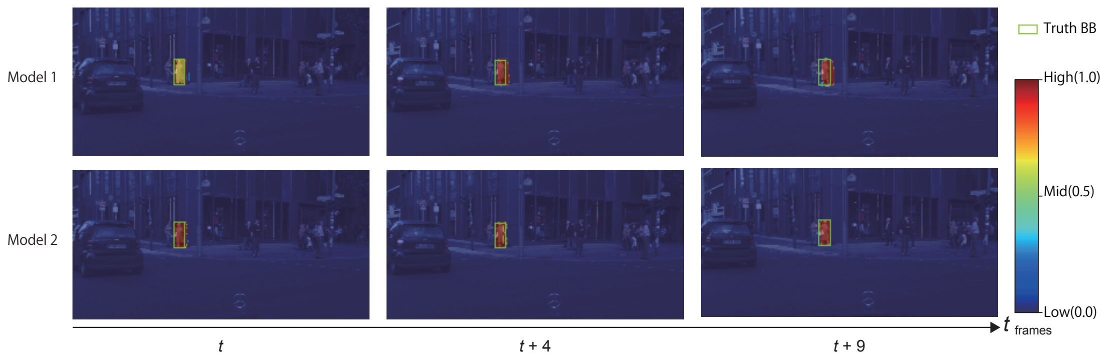

Figure 7: Prediction results of one-person prediction on Cityscapes dataset.

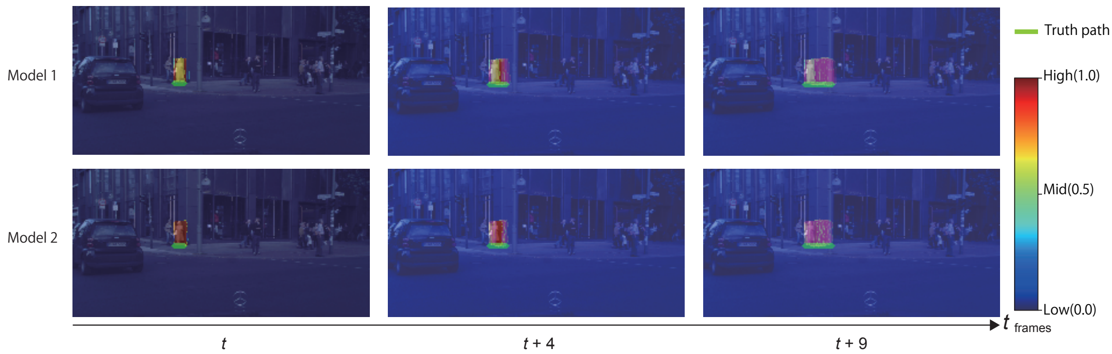

Figure 8: Path prediction results of one-person prediction on Cityscapes dataset.

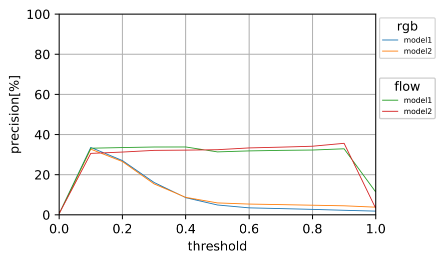

(a)

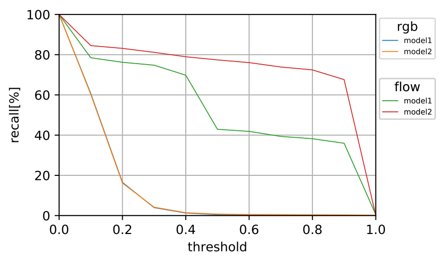

(b)

Figure 9: (a) Precision and (b) recall rates of multi-person prediction on Cityscapes dataset.

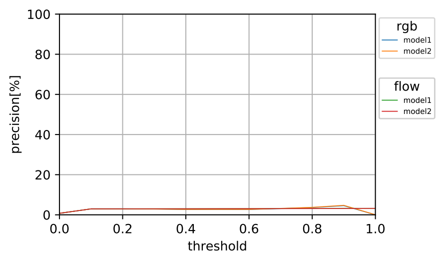

(a)

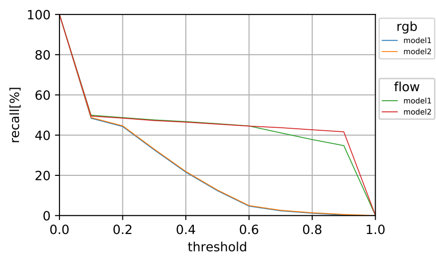

(b)

Figure 10: (a) Precision and (b) recall rates of multi-person prediction on Town Centre dataset.

in time sequence as shown in Figure11, 13. The reason for the results seems to be that the learning features in the encoder have disappeared in the predictor as time has progressed. In using Cityscapes dataset, model 2 predict high probability in the first prediction compared to model 1. Predicted paths are overlap each other in progressing time, as show in Figure 12. However, paths are predicted low probability in model 1. On the other hand, model 2 is able to predict high probability until the last prediction time. The model 2 using Town Centre dataset are also higher prediction than model 1 in the first prediction time, as shown Figure 13. Figure 14 shows all models are predictable along each the truth path. From the above results, recursive model (model2) can predict better than non-recursive model (model 1).

5 CONCLUSIONS

We proposed a probabilistic paths prediction method based on an encoder-predictor model. The proposed method uses context images which visually represents the state and movement of people's positions. The conventional encoder-predictor model applies to images generation. We applied it to paths prediction with expressing probability distribution. We made context images for getting effective information, and evaluated two types of images and two models in one-person and multi-person prediction. The experimental results show optical flow image can get better values than RGB images. And we also show that model 2, which input the last image of encoder and recursively input images in predictor, is better than a non-recursive model. Our future work includes planning to predict individual paths in multi-person prediction.

REFERENCES

Adam, H. and Jules, L. (2019). Megapixels: Origins, ethics, and privacy implications of publicly available face recognition image datasets.

Bazzani, L., Larochelle, H., and Torresani, L. (2017). Recurrent mixture density network for spatiotemporal visual attention. In *ICLR*.

Bhattacharyya, A., Fritz, M., and Schiele, B. (2017). Long-term on-board prediction of people in traffic scenes under uncertainty. In *CVPR*.

Cordts, M., Omran, M., Ramos, S., Rehfeld, T., Enzweiler, M., Beneson, R., Franke, U., Roth, S., and Schiele, B. (2016). The cityscapes dataset for semantic urban scene understanding. In *CVPR*.

Deo, N. and Trivedi, M. (2018). Convolutional social pooling for vehicle trajectory prediction. In *CVPR Workshops*.

Du, X., Vasudevan, R., and Johnson-Roberson, M. (2018). Bio-lstm: A biomechanically inspired recurrent neural network for 3d pedestrian pose and gait prediction. In *RA-L*.

Fukui, H., Hirakawa, T., Yamashita, T., and Fujiyoshi, H. (2019). Attention branch network: Learning of attention mechanism for visual explanation. In *CVPR*.

Hinton, G. and Salakhutdinov, R. (2006). Reducing the dimensionality of data with neural networks. *Science*.

Hochreiter, S. and Schmidhuber, J. (1997). Long short-term memory. *Neural computation*.

Hsieh, J., Liu, B., Huang, D., Fei-Fei, L., and Niebles, J. (2018). Learning to decompose and disentangle representations for video prediction. In *NeurIPS*.

Ilg, E., Mayer, N., Saikia, T., Keuper, M., Dosovitskiy, A., and Brox, T. (2017). Flownet 2.0: Evolution of optical flow estimation with deep networks. In *CVPR*.

Kooij, J., schneider, N., Flohr, F., and Gavrila, D. M. (2014). Context-based pedestrian path prediction. In *ECCV*.

Kozuka, K. and Niebles, J. (2017). Risky region localization with point supervision. In *ICCV Workshops*.

Luc, P., Couprie, C., LeCun, Y., and Verbeek, J. (2018). Predicting future instance segmentation by forecasting convolutional features. In *ECCV*.

Makansi, O., Ilg, E., Çiçek, Ö., and Brox, T. (2019). Overcoming limitations of mixture density networks: A sampling and fitting framework for multimodal future prediction. In *CVPR*.

Palazzi, A., Abati, D., Calderara, S., Solera, F., and Cucchiara, R. (2017). Predicting the driver's focus of attention: the dr(eye)ve project. *Transactions on Pattern Analysis and Machine Intelligence*.

Rehder, E., Wirth, F., Lauer, M., and Stiller, C. (2017). Pedestrian prediction by planning using deep neural networks. *arXiv preprint arXiv:1706.05904*.

Shi, X., Chen, Z., Wang, H., Yeung, D., Wong, W., and Woo, W. (2015). Convolutional lstm network: A machine learning approach for precipitation nowcasting. In *Advances in Neural Information Processing Systems 28*. Curran Associates, Inc.

Tang, S., Andres, B., Andriluka, M., and Schiele, B. (2016). Multi-person tracking by multicut and deep matching. In *ECCV Workshop*.

Tran, D., Bourdev, L., Fergus, R., Torresani, L., and Paluri, M. (2015). Learning spatiotemporal features with 3d convolutional networks. In *ICCV*.

Xu, K., Ba, J., Kiros, R., Cho, K., Courville, A., Salakhudinov, R., Zemel, R., and Bengio, Y. (2015). Show, attend and tell: Neural image caption generation with visual attention. In *Proceedings of the 32nd International Conference on Machine Learning*.

Zeng, K., Chou, S., Chan, F., J. Niebles, J., and Sun, M. (2017a). Agent-centric risk assessment: Accident anticipation and risky region localization. In *CVPR*.

Zeng, K., Shen, W., Huang, D., Sun, M., and Niebles, J. C. (2017b). Visual forecasting by imitating dynamics in natural sequences. In *ICCV*.

Zhang, P., Ouyang, W., Zhang, P., Xue, J., and Zhen, N. (2019). Sr-lstm: State refinement for lstm towards pedestrian trajectory prediction. In *CVPR*.

Zhang, S., Benenson, R., and Schiele, B. (2017). Citypersons: A diverse dataset for pedestrian detection. In *CVPR*.

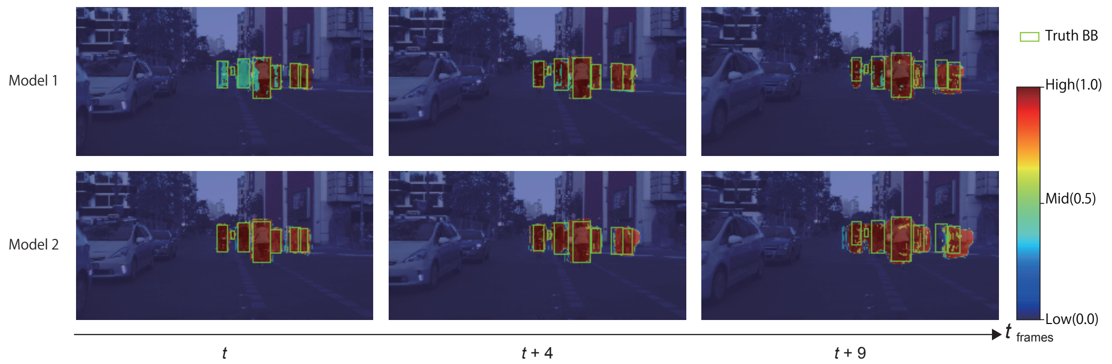

Figure 11: Prediction results of multi-person prediction on Cityscapes dataset.

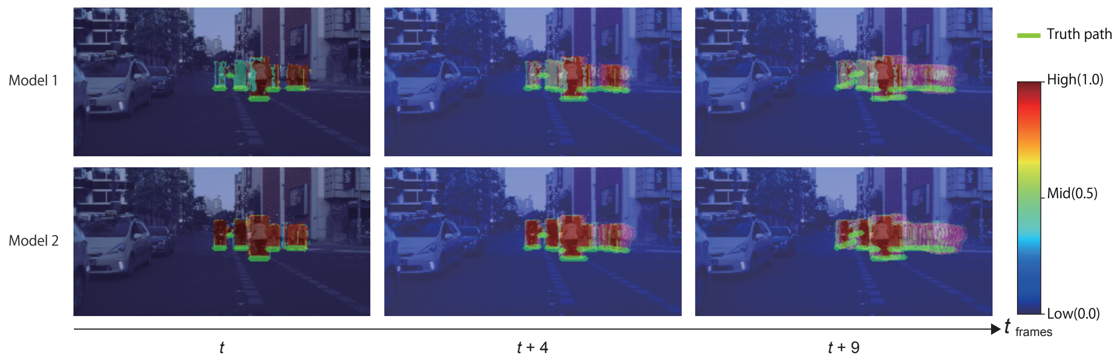

Figure 12: Path prediction results of multi-person prediction on Cityscapes dataset.

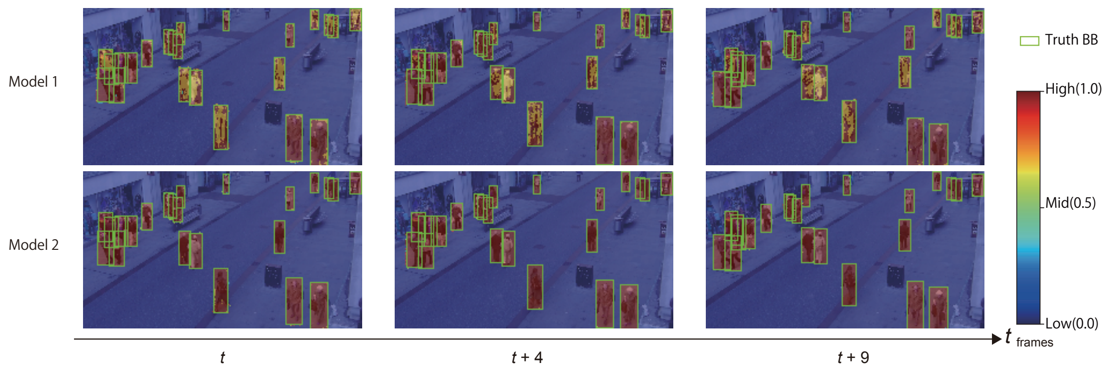

Figure 13: Prediction results of multi-person prediction on Town Centre dataset.

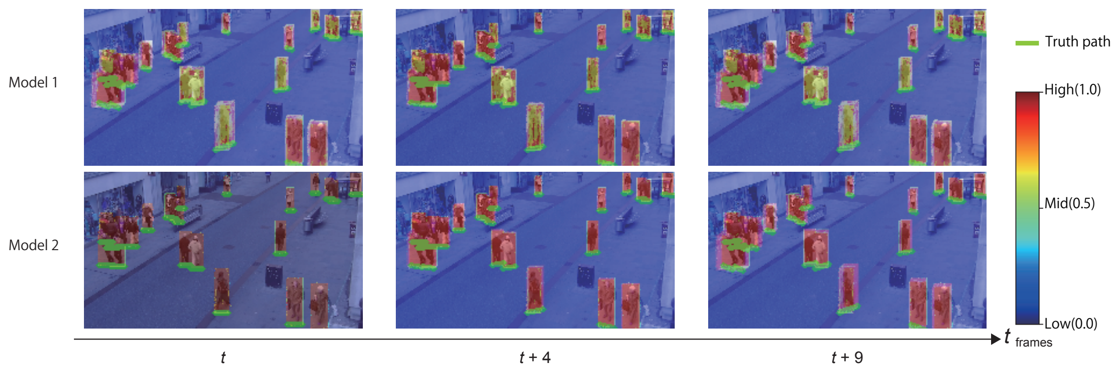

Figure 14: Path prediction results of multi-person prediction on Town Centre dataset.